Engineering a Photoenzyme to Use Red Light

Jose M. Carceller[1,2+], Bhumika Jayee[3+], Claire G. Page[1,2], Daniel G. Oblinsky[1], Nithin Chintala[3], Gustavo Mondragón-Solórzano[3], Jingzhe Cao[1,2], Zayed Alassad[1], Zheyu Zhang[3], Nathaniel White[3], Gregory D. Scholes*[1], Sijia S. Dong*[3,4], Todd K. Hyster*[1,2]

[1] Department of Chemistry, Princeton University, Princeton, New Jersey 08544, United States

[2] Department of Chemistry and Chemical Biology, Cornell University, Ithaca, New York 14853, United States

[3] Department of Chemistry and Chemical Biology, Northeastern University, Boston, Massachusetts 02115, United States

[4] Department of Physics and Department of Chemical Engineering, Northeastern University, Boston, Massachusetts 02115, United States

ABSTRACT: Photoenzymatic catalysis is an emerging platform for asymmetric synthesis. In most of these reactions, the protein templates a charge transfer complex between the cofactor and substrate, which absorbs in the blue region of the electromagnetic spectrum. Here, we report the engineering of a photoenzymatic 'ene'-reductase to utilize red light (620 nm) for a radical cyclization reaction. Mechanistic studies indicate that red light activity is achieved by introducing a broadly absorbing shoulder off the previously identified cyan absorption feature. Molecular dynamics simulations, docking, and excited-state calculations suggest that red light absorption is a $\pi \rightarrow \pi^*$ transition from flavin to the substrate, while the cyan feature is the red-shift of the flavin $\pi \rightarrow \pi^*$ transition, which occurs upon substrate binding. Differences in the excitation event help to disfavor alkylation of the flavin cofactor, a pathway for catalyst decomposition observed with cyan light but not red.

Photochemical transformations have revolutionized organic chemical synthesis by offering a mild strategy for generating radical intermediates.[1–3] Common photocatalysts absorb most strongly in the blue or near-UV region, infusing 63-73 kcal/mol of energy into the reaction. While this is sufficient to facilitate many different bond-making/breaking events, it is more than is required for many chemical transformations. Excess energy can decrease the selectivity for the desired transformation, leading to unwanted side products and catalyst decomposition. These limitations can be overcome using lower-energy red or near-infrared light.[4]

There are a few strategies for utilizing longer wavelengths of light for synthetic organic reactions. Developing red-light absorbing photocatalysts is a straightforward strategy, however, these catalysts often have a more limited redox window compared to their blue-light congeners (Figure 1a).[5–9] Photon upconversion, where select sensitizer and annihilator molecules enable the conversion of two red photons into a single blue one, allows for common blue light photocatalysts with red light irradiation (Figure 1b).[10] Finally, inspired by Z-schemes from nature, a photoinduced electron transfer or energy transfer event is initiated using red light to generate a new red-light absorbing species with enhanced redox properties by comparison to reactions that involve only a single excitation event (Figure 1c).[11,12]

Electron donor-acceptor (EDA) complexes, which involve ground-state association between electron-rich and electron-poor molecules, are common chromophores for photochemical reactions.[13,14] These complexes are attractive because they do not require exogenous photocatalysts, however, red-shifting their absorption is difficult without changing the steric and electronic characteristics of the substrates. Over the past several years, our group and others demonstrated that enzymes could template charge transfer (CT) complexes between biological cofactors and organic substrates.[15–21] When photoexcited, these flavin- and nicotinamide-dependent enzymes can initiate radical reactions. Moreover, the active sites of these proteins can be engineered to improve activity, selectivity, and quantum efficiency.[22] Based on the versatility of this catalyst scaffold, we questioned whether these enzymes could be engineered to red shift the absorption of the CT complex, which typically absorb between 470-510 nm. As described by Mulliken, the absorption of a CT complex can be described using the following equation:

$$h\upsilon_{CT} = IP - EA - \omega$$

where IP = ionization potential of the donor, EA = electron affinity of the acceptor; and ω is the columbic attraction

between the two molecules.[23,24] As protein engineering can influence all three components of this equation, we hypothesized that running a protein engineering campaign

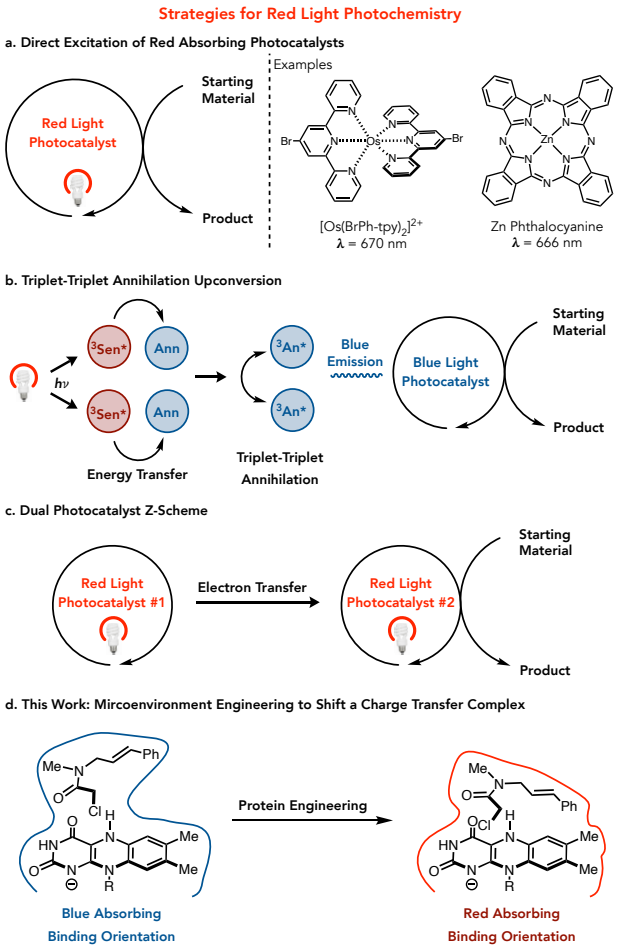

Figure 1. Red-Shifting Complex Absorption

with selection for improved red-light activity should result in a new absorption feature in the red region.[25] Using red light could improve the performance of the photoenzyme by avoiding catalyst degradation through thermal decomposition or cofactor alkylation.

As a model system to test this hypothesis, we examined the radical cyclization of α-chloroamides to produce γ-lactams using the 'ene'-reductase from Gluconobacter oxydans (GluER) as a catalyst. Our previous studies revealed that the unmutated enzyme could catalyze this reaction in 2% yield when irradiated with 630 nm LEDs.[26] We modified the reaction conditions to use protein lysate with 5.5 g/L substrate concentration. Reactions were irradiated with a 620 nm LED at two different light intensities (4273 and 42.73 μmol/cm²). At low light intensities, trace product formation was observed with red light, however, at high intensity, the yield increased to 19% yield. Screening other in-house GluER variants identified GluER-G6 (GluER-T36A-K317M-Y343F) as the best variant, forming product in 58% yield with high light intensity. GluER-G6 had

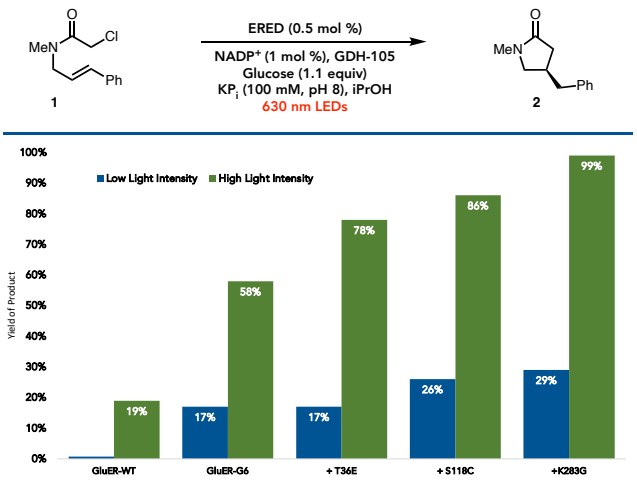

Figure 2. Protein Engineering for Improved Red-Light Activity

previously been engineered for improved quantum efficiency for the cyclization.

To improve upon this starting point, we mutations predicted by MūtCompute, a three-dimensional self-supervised, convolutional neural network, which were previously identied for an enzyme engineered to catalyze an asymmetric alkene hydroalkylation.[27–29] We found that mutating threonine 36 to aspartic acid (T36E), increased the yield to 78% with no change in the enantioselectivity of the transformation. Mutation of serine at position 118 to cystine (S118C) led to product formation in 86% yield. When testing this variant at different substrate concentrations, we observed decreased activity at concentrations above 10 g/L. As the substrate is a weak electrophile, we hypothesized that alkylation of nucleophile side chains was leading to a loss in protein activity. Using proteomic mass spectrometry, we identified the sites of alkylation and targeted them for site saturation mutagenesis. This campaign revealed mutation of lysine at position to 283 to glycine (K283G) provided a variant that provided product in 99% yield with 98:2 er. Total catalyst turnovers were consistent across different catalyst loadings, indicating that increased substrate concentration by comparison to enzyme did not significantly alter the enzymes performance. Increasing the substrate loading to 10 g/L resulted in only a modest decrease in yield (71%). The substrate loading

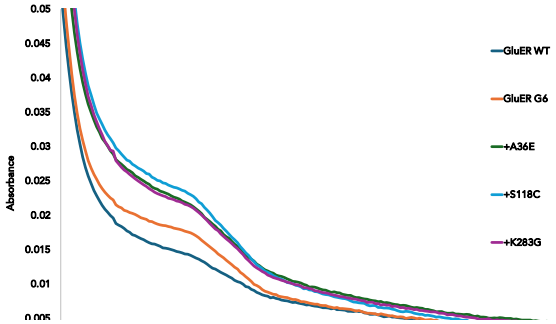

Figure 3. Changes in the CT Complex Over the Protein Engineering Campaign

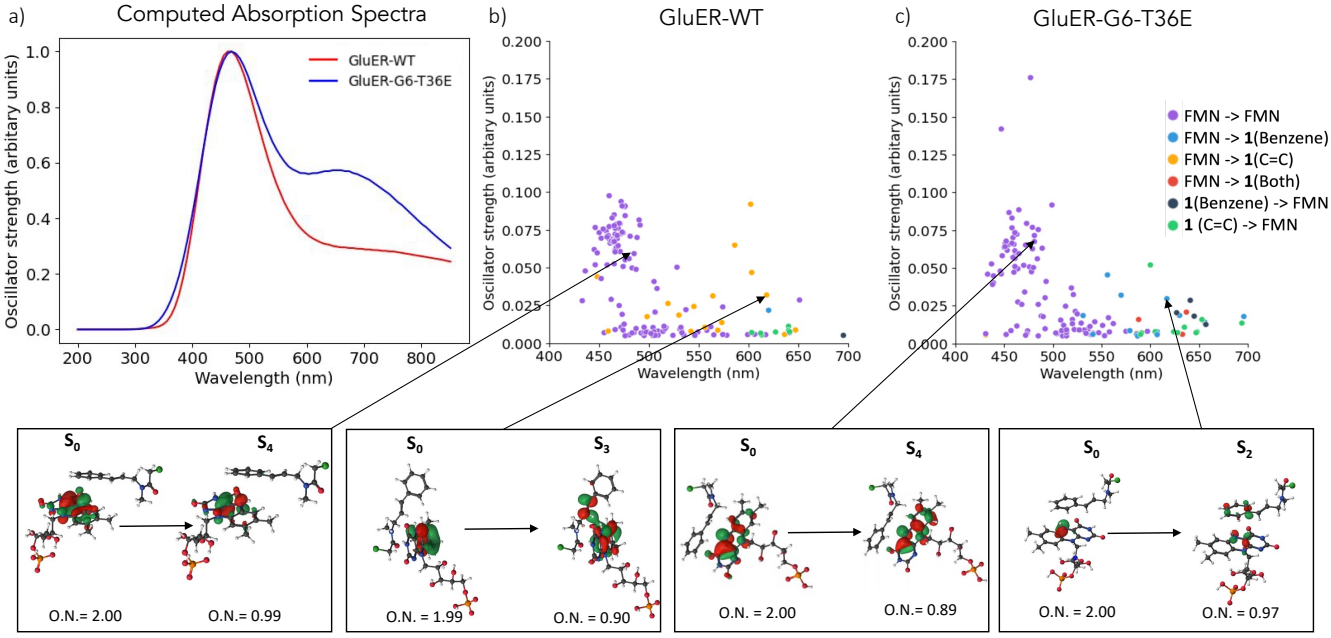

Figure 4. a) Computed absorption spectra considering all GluER-WT and GluER-G6-T36E conformations. b)&c) Distribution of absorption wavelengths, oscillator strengths, and the corresponding transition characters across different conformations of the FMN_{hq}-**1** complex in b) GluER-WT and c) GluER-G6-T36E. Example cyan-light-absorbing transitions and red-light-absorbing transitions are also shown. O.N.: occupation numbers.

could be further increased to 50 g/L, albeit with significantly decreased yield (31%). Interestingly, the final variant of the engineering campaign displayed low level activity with near infrared light (31% yield, 98:2 er), highlighting the opportunity to further red-shift the absorption of the complex.

With an improved variant in hand, we conducted UV-vis experiments across the evolutionary series to determine the changes to the absorption of the charge transfer complex at low substrate concentration to avoid substrate precipitation (3 mM). Using wild-type GluER (0.2 mM), we observe a weakly absorbing complex with the strongest absorption in the cyan region. When moving across the evolutionary series, we find that the cyan absorption feature increases with the best variant from the final three rounds displaying similar magnitude of absorption. The evolution series also results in an absorption should between 550nm and 700nm which increases in magnitude throughout the evolutionary series with the final two variants displaying weak absorption out to 800 nms. We attribute the increase in absorption due to this shoulder between 550 and 800 nm as being responsible for the red light activity.

It is apparent from the UV-vis spectroscopy that mutations to the protein influence absorption features of the enzyme-templated CT complex. To gain a better understanding of how the mutations alter the complexes and their photochemical properties, we first performed molecular dynamics (MD) simulations on the wild-type (WT) GluER and GluER-G6-T36E. We performed molecular docking of **1** to the representative protein conformations from the MD trajectories. We then computed the lowest five electronic states of the ⊂FMN_{hq}-**1** complex using multiconfiguration pair-density functional theory (MC-PDFT) on 260 ⊂FMN_{hq}-**1** conformations for the GluER-WT and 232 conformations for GluER-G6-T36E.[30,31] MC-PDFT is a multi-reference method that has been shown to have similar accuracy as complete active space 2nd-order perturbation theory (CASPT2) and can describe charge transfer excitations with reasonable accuracy while being less computationally expensive than CASPT2.[32] The computed absorption spectra are qualitatively consistent with the UV-vis spectroscopy experiments. GluER-WT and GluER-G6-T36E both absorb strongly in the blue/cyan region whereas GluER-G6-T36E absorbs more strongly than GluER-WT in the red region (Figure 4a). Further analysis of the electronic transitions associated with these bonding conformations revealed that most absorptions in the blue/cyan region involve $\pi \rightarrow \pi^*$ of molecular orbitals (MOs) on FMN_{hq}. Importantly, the lowest-energy bright state of FMN_{hq} alone is 373 nm (Figure S2) indicating that the presence of α-chloroamide **1** red-shifts these excitations. In contrast, electron transitions in the red region involve π MOs of FMN_{hq} and the π^* of α-chloroamide **1** which is consistent with a traditional CT complex (Figure 4b&c insets). To investigate the role of the surrounding amino acids in the CT, we performed additional MC-PDFT calculations considering the sidechains of the aromatic amino acids within the active site, namely W66, W100, and Y177, together with FMN_{hq} and **1**. This showed that the amino acid π^* MOs can be involved in the blue/cyan light transitions by stabilizing the CT state via π stacking interactions, while for red light absorption the CT state from the FMN_{hq} to **1** takes place without any contribution of the aromatic amino acid sidechains (Figures S3 and S4). However, the oscillator strength (*f*) values of the blue/cyan light transitions corresponding to

those transitions where the amino acid MOs are involved are ten to hundred times lower than those where the transitions are within the FMN_{hq} π system, indicating that the most populated transitions upon the absorption of cyan/blue light are the $\pi \rightarrow \pi^*$ transitions within FMN_{hq}.

There is no single, apparent structural descriptor that pinpoints conformations that have red-light absorbing transitions, but overall, the ensemble of conformations that absorb in the red region have a narrower range of distances between the π system of FMN_{hq} and the π system of **1**, where the maximum distance is smaller and the minimum distance is higher, than the ensemble of conformations that have blue/cyan-light absorbing transitions. This is more prominent in GluER-G6-T36E than GluER-WT.

To further understand the effect that mutations have on catalyst turnover numbers and reaction yield, we performed MD simulations of the protein without the α-chloroamide **1** substrate for two additional variants, GluER-G6 and GluER-G6-T36E-S118C-K283G. Analysis of the MD trajectories of GluER-WT, GluER-G6, GluER-G6-T36E, and GluER-G6-T36E-S118C-K283G indicate differences in the conformation flexibility of the protein as determined by radius of gyration (R_g) and the solvent accessible surface area (SASA) of the protein (Figures S5 and S6). Mutations that lead to increased activity also reduce the root mean square fluctuation (RMSF) of residues Y130, C234, and F269 (Figure S7). Addition of these mutations also leads to a decrease in R_g and SASA. These data suggest that reduction of the size and flexibility of the protein active site leads to substrate binding conformations that favor the $FMN_{hq} \rightarrow$ **1** transition required for red light activity.

Finally, to highlight the scalability of this red light-initiated photochemistry, we tested reactions a different reaction scales using cyan and red LEDs. On reaction scales ranging from 10 mg to 10 grams, red light irradiated reactions provided product in yields of 82 to 92% (Figure 5). In contrast, when using cyan LEDs, the yields are lowest at 10 mg scale (21%) and increases to 70% at 5-gram scale. The suppressed yields on small scale suggested that the protein was decomposing. To probe thermal denaturing of the protein, we tested differences in reaction temperature at various points. While the reaction irradiated with red light was 2-8 ºC lower in temperature than the reaction with cyan light, the temperature was still 25 ºC below the melting point of the enzyme, suggesting that thermal denaturing was not responsible for the yield differences. Instead, we noticed a color difference at the end of the two reactions, with the red-light reaction being yellow/orange while the cyan reaction was white. Based on previous reports, this difference could be due to possible alkylation of the flavin cofactor.[33–36] After removing the remaining small molecules, denaturing the protein and subjecting the reaction to high resolution mass spectrometry, we identified a mass consistent with double alkylation of the flavin cofactor by the substrate. Importantly, this mass is only observed in the reaction irradiated with cyan light. Based on these results, we hypothesized that the binding conformation responsible for red light activity with the alkene packed over the flavin cofactor helps to disfavor flavin alkylation. This observation indicates that future reaction development could be enhanced by using red light as this will ensure prolonged catalyst lifetimes (Figure 5).

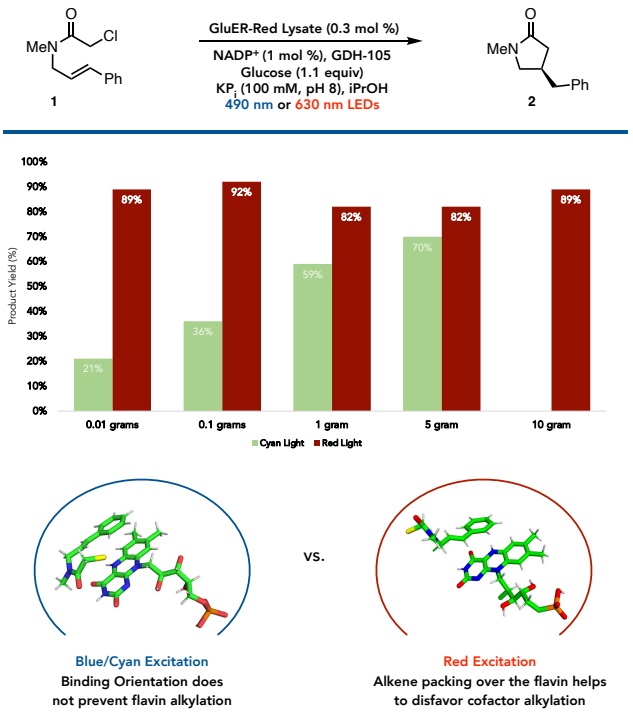

Figure 5. Reactions at different scales and rationale for flavin alkylation catalyst deactivation

In summary, we have engineered a flavin-dependent photoenzyme to utilize red-light excitation for radical initiation. This work highlights the opportunity to tune the microenvironment of the protein to alter the characteristics of charge transfer complexes. Computation studies indicate that excitations in the cyan region primarily involve orbitals on flavin, while red light excitation involves orbitals on the flavin and the substrate. Moreover, differences in the binding orientations responsible for red absorption features help to avoid flavin alkylation and extend the radical lifetime. Overall, this study highlights an opportunity to use wavelength engineering to access improved photoenzymes.

ASSOCIATED CONTENT

Supporting Information

The Supporting Information is available free of charge at https://pubs.acs.org Experimental procedures and

Author Contributions

+ JMC and BJ contributed equally

characterization data, including supplemental figures sX-sXX and Supplemental Tables X-X.

AUTHOR INFORMATION

Corresponding Author

* Todd K. Hyster – Department of Chemistry, Princeton University, Princeton, New Jersey 08544, United States. Email: thyster@princeton.edu
* Sijia S. Dong – Department of Chemistry and Chemical Biology, Northeastern University, Boston, MA 02115, United States. Email: s.dong@northeastern.edu
* Greogry D. Scholes – Department of Chemistry, Princeton University, Princeton, New Jersey 08544, United States. Email: gscholes@princeton.edu

Funding Sources

This work was supported by BioLEC, an Energy Frontier Research Center funded by the U.S. Department of Energy, Office of Science, Basic Energy Sciences under Award #DE-SC0019370. The work performed at Northeastern University used computing resources of Northeastern University Research Computing and the National Energy Research Scientific Computing Center (NERSC), a Department of Energy Office of Science User Facility using NERSC award BES-ERCAP0026704 and BES-ERCAP0026375. Development of computational tools and protocols used in this work was supported by Northeastern University startup funds. CGP is supported by an NSF-GFRP. DGO is supported by a NSERC graduate fellowship.

ACKNOWLEDGMENT

We thank the Stache lab for use of their infrared camera.

REFERENCES

(1) Shaw, M. H.; Twilton, J.; MacMillan, D. W. C. Photoredox Catalysis in Organic Chemistry. *J. Org. Chem.* **2016**, *81* (16), 6898–6926. https://doi.org/10.1021/acs.joc.6b01449.

(2) Romero, N. A.; Nicewicz, D. A. Organic Photoredox Catalysis. *Chem. Rev.* **2016**, *116* (17), 10075–10166. https://doi.org/10.1021/acs.chemrev.6b00057.

(3) Prier, C. K.; Rankic, D. A.; MacMillan, D. W. C. Visible Light Photoredox Catalysis with Transition Metal Complexes: Applications in Organic Synthesis. *Chem. Rev.* **2013**, *113* (7), 5322–5363. https://doi.org/10.1021/cr300503r.

(4) Schade, A. H.; Mei, L. Applications of Red Light Photoredox Catalysis in Organic Synthesis. *Org. Biomol. Chem.* **2023**, *21* (12), 2472–2485. https://doi.org/10.1039/d3ob00107e.

(5) Katsurayama, Y.; Ikabata, Y.; Maeda, H.; Segi, M.; Nakai, H.; Furuyama, T. Direct Near Infrared Light–Activatable Phthalocyanine Catalysts. *Chem. A Eur. J.* **2022**, *28* (2), e202103223. https://doi.org/10.1002/chem.202103223.

(6) Ravetz, B. D.; Tay, N. E. S.; Joe, C. L.; Sezen-Edmonds, M.; Schmidt, M. A.; Tan, Y.; Janey, J. M.; Eastgate, M. D.; Rovis, T. Development of a Platform for Near-Infrared Photoredox Catalysis. *ACS Cent. Sci.* **2020**, *6* (11), 2053–2059. https://doi.org/10.1021/acscentsci.0c00948.

(7) Sellet, N.; Sebbat, M.; Elhabiri, M.; Cormier, M.; Goddard, J.-P. Squaraines as Near-Infrared Photocatalysts for Organic Reactions. *Chem. Commun.* **2022**, *58* (99), 13759–13762. https://doi.org/10.1039/d2cc04707a.

(8) Goldschmid, S. L.; Bednářová, E.; Beck, L. R.; Xie, K.; Tay, N. E. S.; Ravetz, B. D.; Li, J.; Joe, C. L.; Rovis, T. Tuning the Electrochemical and Photophysical Properties of Osmium-Based Photoredox Catalysts. *Synlett* **2022**, *33* (03), 247–258. https://doi.org/10.1055/s-0041-1737792.

(9) Goldschmid, S. L.; Tay, N. E. S.; Joe, C. L.; Lainhart, B. C.; Sherwood, T. C.; Simmons, E. M.; Sezen-Edmonds, M.; Rovis, T. Overcoming Photochemical Limitations in Metallaphotoredox Catalysis: Red-Light-Driven C–N Cross-Coupling. *J. Am. Chem. Soc.* **2022**, *144* (49), 22409–22415. https://doi.org/10.1021/jacs.2c09745.

(10) Ravetz, B. D.; Pun, A. B.; Churchill, E. M.; Congreve, D. N.; Rovis, T.; Campos, L. M. Photoredox Catalysis Using Infrared Light via Triplet Fusion Upconversion. *Nature* **2019**, *565* (7739), 343–346. https://doi.org/10.1038/s41586-018-0835-2.

(11) Glaser, F.; Wenger, O. S. Red Light-Based Dual Photoredox Strategy Resembling the Z-Scheme of Natural Photosynthesis. *JACS Au* **2022**, *2* (6), 1488–1503. https://doi.org/10.1021/jacsau.2c00265.

(12) Fajardo, J.; Barth, A. T.; Morales, M.; Takase, M. K.; Winkler, J. R.; Gray, H. B. Photoredox Catalysis Mediated by Tungsten(0) Arylisocyanides. *J. Am. Chem. Soc.* **2021**, *143* (46), 19389–19398. https://doi.org/10.1021/jacs.1c07617.

(13) Lima, C. G. S.; Lima, T. de M.; Duarte, M.; Jurberg, I. D.; Paixão, M. W. Organic Synthesis Enabled by Light-Irradiation of EDA Complexes: Theoretical Background and Synthetic Applications. *ACS Catal.* **2016**, *6* (3), 1389–1407. https://doi.org/10.1021/acscatal.5b02386.

(14) Crisenza, G. E. M.; Mazzarella, D.; Melchiorre, P. Synthetic Methods Driven by the Photoactivity of Electron Donor–Acceptor Complexes. *J. Am. Chem. Soc.* **2020**, *142* (12), 5461–5476. https://doi.org/10.1021/jacs.0c01416.

(15) Emmanuel, M. A.; Greenberg, N. R.; Oblinsky, D. G.; Hyster, T. K. Accessing Non-Natural Reactivity by Irradiating Nicotinamide-Dependent Enzymes with Light. *Nature* **2016**, *540* (7633), 414–417. https://doi.org/10.1038/nature20569.

(16) Fu, H.; Cao, J.; Qiao, T.; Qi, Y.; Charnock, S. J.; Garfinkle, S.; Hyster, T. K. An Asymmetric Sp3-Sp3 Cross-Electrophile Coupling Using 'Ene'-Reductases. *Nature* **2022**, *610* (7931), 302–307. https://doi.org/10.1038/s41586-022-05167-1.

(17) Clayman, P. D.; Hyster, T. K. Photoenzymatic Generation of Unstabilized Alkyl Radicals: An Asymmetric Reductive

Cyclization. *J. Am. Chem. Soc.* **2020**, *142* (37), 15673–15677. https://doi.org/10.1021/jacs.0c07918.

(18) Gao, X.; Turek-Herman, J. R.; Choi, Y. J.; Cohen, R. D.; Hyster, T. K. Photoenzymatic Synthesis of α-Tertiary Amines by Engineered Flavin-Dependent "Ene"-Reductases. *J. Am. Chem. Soc.* **2021**, *143* (47), 19643–19647. https://doi.org/10.1021/jacs.1c09828.

(19) Page, C. G.; Cooper, S. J.; DeHovitz, J. S.; Oblinsky, D. G.; Biegasiewicz, K. F.; Antropow, A. H.; Armbrust, K. W.; Ellis, J. M.; Hamann, L. G.; Horn, E. J.; Oberg, K. M.; Scholes, G. D.; Hyster, T. K. Quaternary Charge-Transfer Complex Enables Photoenzymatic Intermolecular Hydroalkylation of Olefins. *J. Am. Chem. Soc.* **2020**, *143* (1), 97–102. https://doi.org/10.1021/jacs.0c11462.

(20) Laguerre, N.; Riehl, P. S.; Oblinsky, D. G.; Emmanuel, M. A.; Black, M. J.; Scholes, G. D.; Hyster, T. K. Radical Termination via B-Scission Enables Photoenzymatic Allylic Alkylation Using "Ene"-Reductases. *ACS Catal.* **2022**, *12* (15), 9801–9805. https://doi.org/10.1021/acscatal.2c02294.

(21) Turek-Herman, J. R.; Rosenberger, M.; Hyster, T. K. Synthesis of B-Quaternary Lactams Using Photoenzymatic Catalysis. *Asian J. Org. Chem.* **2023**, *12* (8). https://doi.org/10.1002/ajoc.202300274.

(22) Nicholls, B. T.; Oblinsky, D. G.; Kurtoic, S. I.; Grosheva, D.; Ye, Y.; Scholes, G. D.; Hyster, T. K. Engineering a Non-Natural Photoenzyme for Improved Photon Efficiency**. *Angew. Chem. Int. Ed.* **2022**, *61* (2), e202113842. https://doi.org/10.1002/anie.202113842.

(23) Rosokha, S. V.; Kochi, J. K. Fresh Look at Electron-Transfer Mechanisms via the Donor/Acceptor Bindings in the Critical Encounter Complex. *Acc. Chem. Res.* **2008**, *41* (5), 641–653. https://doi.org/10.1021/ar700256a.

(24) Mulliken, R. S. Structures of Complexes Formed by Halogen Molecules with Aromatic and with Oxygenated Solvents 1. *J. Am. Chem. Soc.* **1950**, *72* (1), 600–608. https://doi.org/10.1021/ja01157a151.

(25) Page, C. G.; Cao, J.; Oblinsky, D. G.; MacMillan, S. N.; Dahagam, S.; Lloyd, R. M.; Charnock, S. J.; Scholes, G. D.; Hyster, T. K. Regioselective Radical Alkylation of Arenes Using Evolved Photoenzymes. *J. Am. Chem. Soc.* **2023**, *145* (21), 11866–11874. https://doi.org/10.1021/jacs.3c03607.

(26) Biegasiewicz, K. F.; Cooper, S. J.; Gao, X.; Oblinsky, D. G.; Kim, J. H.; Garfinkle, S. E.; Joyce, L. A.; Sandoval, B. A.; Scholes, G. D.; Hyster, T. K. Photoexcitation of Flavoenzymes Enables a Stereoselective Radical Cyclization. *Science* **2019**, *364* (6446), 1166–1169. https://doi.org/10.1126/science.aaw1143.

(27) Liu, Y.; Bender, S. G.; Sorigue, D.; Diaz, D. J.; Ellington, A. D.; Mann, G.; Allmendinger, S.; Hyster, T. K. Asymmetric Synthesis of A-Chloroamides via Photoenzymatic Hydroalkylation of Olefins. *J. Am. Chem. Soc.* **2024**. https://doi.org/10.1021/jacs.4c00927.

(28) d'Oelsnitz, S.; Diaz, D. J.; Kim, W.; Acosta, D. J.; Dangerfield, T. L.; Schechter, M. W.; Minus, M. B.; Howard, J. R.; Do, H.; Loy, J. M.; Alper, H. S.; Zhang, Y. J.; Ellington, A. D. Biosensor and Machine Learning-Aided Engineering of an Amaryllidaceae Enzyme. *Nat. Commun.* **2024**, *15* (1), 2084. https://doi.org/10.1038/s41467-024-46356-y.

(29) Shroff, R.; Cole, A. W.; Diaz, D. J.; Morrow, B. R.; Donnell, I.; Annapareddy, A.; Gollihar, J.; Ellington, A. D.; Thyer, R. Discovery of Novel Gain-of-Function Mutations Guided by Structure-Based Deep Learning. *ACS Synth. Biol.* **2020**, *9* (11), 2927–2935. https://doi.org/10.1021/acssynbio.0c00345.

(30) Manni, G. L.; Carlson, R. K.; Luo, S.; Ma, D.; Olsen, J.; Truhlar, D. G.; Gagliardi, L. Multiconfiguration Pair-Density Functional Theory. *J. Chem. theory Comput.* **2014**, *10* (9), 3669–3680. https://doi.org/10.1021/ct500483t.

(31) Gagliardi, L.; Truhlar, D. G.; Manni, G. L.; Carlson, R. K.; Hoyer, C. E.; Bao, J. L. Multiconfiguration Pair-Density Functional Theory: A New Way To Treat Strongly Correlated Systems. *Acc. Chem. Res.* **2017**, *50* (1), 66–73. https://doi.org/10.1021/acs.accounts.6b00471.

(32) Andersson, K.; Malmqvist, P. A.; Roos, B. O.; Sadlej, A. J.; Wolinski, K. Second-Order Perturbation Theory with a CASSCF Reference Function. *J. Phys. Chem.* **1990**, *94* (14), 5483–5488. https://doi.org/10.1021/j100377a012.

(33) Ghisla, S.; Massey, V.; Choong, Y. S. Covalent Adducts of Lactate Oxidase. Photochemical Formation and Structure Identification. *J. Biol. Chem.* **1979**, *254* (21), 10662–10669. https://doi.org/10.1016/s0021-9258(19)86571-7.

(34) Walker, Wolfram. H.; Hemmerich, P.; Massey, V. Light-Induced Alkylation and Dealkylation of the Flavin Nucleus. *Eur. J. Biochem.* **1970**, *13* (2), 258–266. https://doi.org/10.1111/j.1432-1033.1970.tb00926.x.

(35) Li, X.; Page, C. G.; Zanetti-Polzi, L.; Kalra, A. P.; Oblinsky, D. G.; Daidone, I.; Hyster, T. K.; Scholes, G. D. Mechanism and Dynamics of Photodecarboxylation Catalyzed by Lactate Monooxygenase. *J. Am. Chem. Soc.* **2023**, *145* (24), 13232–13240. https://doi.org/10.1021/jacs.3c02446.

(36) Page, C. G.; Cooper, S. J.; DeHovitz, J. S.; Oblinsky, D. G.; Biegasiewicz, K. F.; Antropow, A. H.; Armbrust, K. W.; Ellis, J. M.; Hamann, L. G.; Horn, E. J.; Oberg, K. M.; Scholes, G. D.; Hyster, T. K. Quaternary Charge-Transfer Complex Enables Photoenzymatic Intermolecular Hydroalkylation of Olefins. *J. Am. Chem. Soc.* **2020**, *143* (1), 97–102. https://doi.org/10.1021/jacs.0c11462.